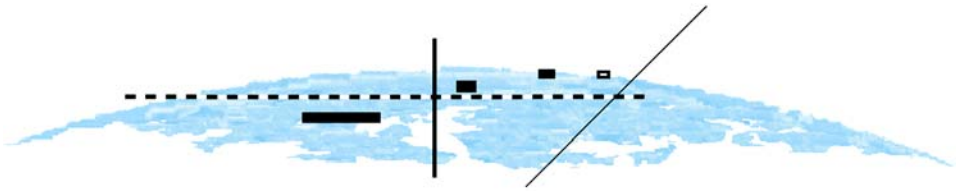

GeoForschungsZentrum Potsdam

STIFTUNG DES ÖFFENTLICHEN RECHTS

Scientific Technical Report

ISSN 1610-0956

Johann Wünsch, Peter Schwintzer, Svetozar Petrović

Comparison of two different ocean tide models especially with respect to the GRACE satellite mission

Scientific Technical Report STR05/08

DOI: 10.2312/GFZ.b103-05088

DOI: 10.2312/GFZ.b103-05088

Preface

At the time when the preparation of this report entered its final phase, the tragic news arrived concerning our colleague and coauthor, Dr. Peter Schwintzer, who suddenly passed away on December 24, 2004. His death is a huge loss, not only for his colleagues, but for the whole scientific community.

Undoubtedly, he would have suggested quite a number of improvements in the final draft of this report.

We are grateful to him for the pleasant cooperation in past years. He will be missed greatly.

J. Wünsch and S. Petrović

GeoForschungsZentrum Potsdam Scientific Technical Report STR 05/08
DOI: 10.2312/GFZ.b103-05088

DOI: 10.2312/GFZ.b103-05088

Abstract

The GRACE dual satellite mission (launched in March, 2002) offers the possibility of computing monthly highly accurate mean gravity fields over an expected lifetime of five years. Unfortunately, the quality of these monthly gravity field products does not yet reach the pre-launch expectations. Possible error sources might be insufficient instrument data processing and parameterization or modeling of short-term atmospheric and oceanic mass variations. Another candidate is the ocean tide model. Especially, incomplete subtraction (de-aliasing) of short period tides may be partially aliased into the monthly gravity field solutions. Therefore, we analyzed the difference of two ocean tide models (FES2004 and CSR 4.0) which are used at the GRACE Science Data System level-2 processing centers at GFZ Potsdam and CSR (Center for Space Research, Austin), respectively, and which may serve as a measure of the ocean tide model error.

We have computed: a) straightforward monthly means of tidal elevation differences and b) simulations of tidal elevation differences at footpoints of GRACE A. The results of a) represent the differences of the monthly means of both tide models with respect to an uniform sampling (grid). The results of b) include the influence of spatially uneven sampling distribution (only along the orbit) and show that for the S_2 and K_2 tidal constituents, aliasing causes effects which cannot be neglected with respect to the presently achievable GRACE measurement accuracy for degrees $n \leq 7$ (S_2) and $n \leq 8$ (K_2).

Key words: time-variable gravity, GRACE satellite mission, ocean tides, aliasing, tidal models.

DOI: 10.2312/GFZ.b103-05088

DOI: 10.2312/GFZ.b103-05088

Contents

DOI: 10.2312/GFZ.b103-05088

DOI: 10.2312/GFZ.b103-05088

1 Introduction: Goals of the GRACE gravity mission

The twin GRACE satellites were launched on March 17, 2002 (GRACE = Gravity Recovery and Climate Experiment). Their primary purpose is to monitor the gravity field of the Earth (Tapley and Reigber 2001), both the static field and the time-variable part of it (Dickey et al. 1997, Wahr et al. 1998, Peters 2001). GRACE is a joint U.S.–German project implemented by NASA and DLR under the NASA Earth System Science Pathfinder Program and has an intended lifetime of 5 years. It uses low–low satellite–to–satellite microwave tracking (both satellites are at a low orbital altitude), see also www.gfz-potsdam.de/grace/ and www.csr.utexas.edu/grace/.

Tapley et al. (2004a) describe: 'The GRACE mission consists of two identical satellites in near-circular orbits at ≈500 km altitude and 89.5° inclination, separated from each other by approximately 220 km along-track, and linked by a highly accurate inter-satellite, K-Band microwave ranging system. Each satellite, in addition to the inter-satellite ranging system, also carries Global Positioning System (GPS) receivers and attitude sensors and high precision accelerometers. The satellite altitude decays naturally (≈30 m/day) so that the ground track does not have a fixed repeat pattern.'

Besides the main general goal of the GRACE mission, recovery of the time-variable gravity field, there are many specific goals which should be mentioned: an extremely accurate static gravity field model (Tapley et al. 2004a, Reigber et al. 2004); deriving geostrophic ocean currents from the static field plus TOPEX/Poseidon (T/P) altimetry (Tapley et al. 2003, Dobslaw et al. 2004); inferring deep ocean currents; studying the seasonal (and interannual) hydrological cycle over the continents (Schmidt et al. 2005, Wahr et al. 2004, Tapley et al. 2004b); verifying the influence of (seasonal) ocean bottom pressure variations in the world ocean on time-variable gravity (Kanzow et al. 2005); verifying the seasonal mass balance of the world ocean (Chambers et al. 2004); testing the inverted barometer assumption (Wunsch and Stammer 1997) for ocean response to atmospheric pressure forcing; improving models of the oceanic pole tide (both at the Chandler period and the annual period); finding secular trends in the gravity field due to postglacial rebound mainly over North America and over Fennoscandia (Velicogna and Wahr 2002); monitoring the mass balance of changing ice sheets over Greenland (Fleming et al. 2004) and over Antarctica and also the mass balance of continental glaciers; determining isostatic gravity anomalies (Kaban et al. 2004); finally: finding the signature of very strong earthquakes in the gravity field (Gross and Chao 2001). Additionally, human-caused gravity signals can also change the Earth's gravity field; as an example let us mention the Three Gorges Dam project in China (Boy and Chao 2002). In short, a continuous monitoring of the Earth's changing

DOI: 10.2312/GFZ.b103-05088

water budget has become inevitable and the era of a systematic survey is approaching.

There are several possible error sources in orbit determination and gravity field determination. A model of *solid* Earth tides has to be considered in the step of orbit determination.

Soil moisture fields on the continents are very difficult to model. Only very recently more advanced numerical soil moisture models have been published (Milly and Shmakin 2002, Döll et al. 2003, Fan and van den Dool 2004), which are still under development. In order to learn about soil moisture using GRACE (Schmidt et al. 2005, Wahr et al. 2004, Tapley et al. 2004b), one has to subtract all other effects, in first place the relatively well-known ocean tidal mass variations, nontidal ocean mass variations and changing atmospheric attraction (modelled by vertical integration) from the GRACE observations. However, all these contributions are subject to at least small modelling errors. High-frequency soil moisture variations are a further source of errors for monthly means (Han et al. 2004, Thompson et al. 2004).

The GRACE dealiasing products are routinely being produced by F. Flechtner, GFZ Potsdam, (AOD = Atmosphere Ocean Dealiasing Product; Flechtner 2003) by using a barotropic ocean circulation model and ECMWF atmospheric data.

Errors of *ocean tide models* are an important topic, as evidenced by comparison with bottom pressure recorders. Especially in the shallow marginal seas, significant ocean tide model errors do occur. In the following, the difference between two ocean tide models (one from Center for Space Research, Austin, Texas, (model CSR 4.0), and one from Le Provost et al., CNES, (model FES2004)) is taken as a measure of the errors of ocean tide models.

DOI: 10.2312/GFZ.b103-05088

2 Spatio-temporal aliasing

Monthly mean gravity fields over a 5 years nominal lifetime are expected from the GRACE mission, some of them are already available. All short period variations are aliased into the monthly means (Wiehl and Dietrich 2005) if they are not correctly subtracted ('de-aliased'). These variations include ocean tides, nontidal ocean, atmospheric pressure fields (Thompson et al. 2004) and soil moisture.

In two dictionaries we find the following definitions of 'aliasing':

A) **aliasing:** 'The condition that two or more functions are indistinguishable because they have the same values at a finite set of points. Such functions are said to be aliases of each other. The aliasing problem often occurs in an undersampled discrete Fourier transform' (Morris 1991).

B) **aliasing:** 'A distortion in the frequency of sampled data produced by insufficient sampling per wavelength, which can result in spurious frequencies. When the sampling rate is too low to represent the wave-form accurately, then aliasing will occur. To avoid aliasing, the sampling frequency should be at least twice that of the highest-frequency component contained within the sampled wave-form. (Alternatively, an anti-alias filter can be applied, which removes frequency components above the Nyquist frequency)' (Allaby and Allaby 1999). Both definitions A) and B) appear nearly equivalent.

An example for aliasing is provided by an ≈10 day atmospheric normal mode which has been detected in VLBI polar motion data (Eubanks et al. 1995). This normal mode will not be completely removed in monthly averages.

A further example: Song and Zlotnicki (2004) recently showed with a non-Boussinesq ocean circulation model that baroclinic features like tropical instability waves cause strong ocean bottom pressure fluctuations (around 4-mbar amplitude) with a period of about 30 d. This could possibly alias into the GRACE data, if a model is used for de-aliasing which does not allow for baroclinic dynamics (Kanzow et al. 2005).

The literature on ocean tidal aliasing comprises: Ray et al. (2001), Knudsen and Andersen (2002), Knudsen (2003), Ray et al. (2003) and Han et al. (2004). Ray et al. (2001) first studied the effect of M_2 error on GRACE by averaging 12.4 h of M_2 error for a 3-month averaged GRACE sensitivity. Knudsen and Andersen (2002) calculated the tidal aliasing frequencies for the four most energetic tidal constituents. They computed a monthly mean tidal error by applying convolution in the time domain using a block averaging function with corresponding aliasing periods. In the more realistic investigations (Knudsen 2003, Ray et al. 2003), the authors considered orbital sampling and found sectorial anomalies in the recovered gravity field. Ray et al. (2003) did two kinds of simulations for the two-satellite case. The resulting errors in an estimated monthly geoid range between –2 mm .... +2 mm. Cheng (2002) employed a

DOI: 10.2312/GFZ.b103-05088

semianalytic formulation and modeled the GRACE range-rate observations to study the detailed perturbation spectrum due to ocean tides. Han et al. (2004) transformed the effects of the tidal model error (defined as the difference between CSR 4.0 and the Japanese hydrodynamic model NAO99) into the GRACE potential difference observables (potential difference between GRACE A and B satellites). By inverting these observables, the effects of their temporal variation on the monthly mean gravity field estimates were determined. Han et al. considered orbital sampling and the periods of each tide constituent. They found that a model error in S_2 causes errors 3 times larger than the GRACE measurement noise at degrees n<15 in the monthly gravity solution. Errors in K_1, O_1 and M_2 could be reduced to below the measurement noise level by monthly averaging.

The present study uses both straightforward monthly averages as well as orbital simulations.

Concerning the orbit of GRACE, Knudsen (2003) employs the following argumentation: '*To study the characteristics of the ocean tides as sampled by GRACE in detail, alias frequencies of the eight largest tidal constituents were computed (e.g., Knudsen and Andersen 2002). A sampling interval close to half a sidereal day was assumed. This corresponds to a sampling of the gravity field at both ascending and descending tracks, which will be relevant except for areas near the poles. In the analysis the actual precession of the node was taken into account. Hence, a sampling interval of 0.49846 d was applied. The GRACE satellite will fly in a non-repeating orbit that complicates the definition of alias frequencies, since the sampling will not be regular (Knudsen and Andersen 2002). However, GRACE will measure the gravity field averaged over an area of a few hundred kilometres. Considering such a region the satellite may sample the gravity field several times during a one-month period at times separated by multiples of the assumed sampling frequency.*' (The sampling interval is the time interval after which GRACE traverses a given point on the Earth again).

In the simplest approach to the aliasing phenomenon, we have (e.g., Wilks 1995):

$$f_a = |f_{sampl} - f| \tag{1}$$

where $f_a = 1/P_a$, $f = 1/P$ and $f_{sampl} = 1/P_{sampl}$. Here, f_a is the aliasing frequency (apparent frequency), f is the frequency of the signal (e.g., ocean tide) and f_{sampl} is the sampling frequency. As mentioned above, we assume $P_{sampl} = 0.49846$ d.

Table 1 lists alias periods according to Knudsen (2003). M_2 has an alias frequency of 13.6 d and S_2 has an alias frequency of 162.2 d. N_2 has an alias frequency of 9.1 d and K_2 of 1460 d or 4 a. The diurnal constituents are sampled sufficiently to avoid aliases. However, their frequencies are not identical to the sampling frequency, so a *modulation* of the amplitude will occur. For K_1, O_1, P_1 and Q_1 the amplitudes will be modulated by periods of 2920, 13.6, 9.1 and 9.1 d, respectively.

DOI: 10.2312/GFZ.b103-05088

Table 1: Periods, alias periods, modulation of amplitudes and relative magnitudes for some tidal constituents (Knudsen 2003)

Constituent	Period P [d]	P_a [d]	Modulation [d]	Averaged (convolution)	Averaged (simulation)
M_2	0.5175	13.6	–	0.10	0.07
S_2	0.5000	162.2	–	0.94	0.95
N_2	0.5274	9.1	–	0.08	–
K_2	0.4986	1460	–	1.00	–
K_1	0.9973	0.9969	2920	0.01	0.07
O_1	1.0758	0.9969	13.6	0.01	0.04
P_1	1.0028	0.9969	9.1	0.01	–
Q_1	1.1195	0.9969	9.1	0.01	–

As Knudsen (2003) points out, in the frequency domain a convolution by a block averaging function corresponds to a multiplication by a sinc function ($\mathrm{sinc}(u) = \sin(u)/u$) (Brigham 1992). Using this function together with the above alias frequencies, the magnitudes of the monthly averaged tidal constituents were computed by Knudsen (2003): The effect of averaging GRACE gravity over monthly intervals shows the result that M_2, S_2, N_2 and K_2 tidal errors are reduced to 10%, 94%, 8% and 100% of their original magnitudes, respectively. The errors of S_2 and K_2 are practically unreduced (not averaged to zero) in the GRACE data processing. The diurnal tidal errors are almost fully reduced in this approximation (to around 1%, cf. column 'convolution' in Table 1). A more detailed orbital simulation (column 'simulation' in Table 1) led Knudsen (2003) to reduction factors of 7% and 95% for M_2 and S_2 tidal errors, respectively, of their original magnitudes. However, the K_1 and O_1 errors were reduced to 7% and 4%. This is slightly higher than the $\mathrm{sinc}(u)$ result of 1%. Generally, the solar tides cause more problems for GRACE than the lunar tides (Ray et al. 2003).

DOI: 10.2312/GFZ.b103-05088

3 Gravity perturbations caused by ocean tides

Let us expand the ocean tidal elevations in normalized complex spherical harmonics $Y_n^m(\theta, \lambda)$ according to (Ray et al. 2003):

$$\zeta(\theta, \lambda, t) = \sum_{n,m} z_{nm}(t)\, Y_n^m(\theta, \lambda). \tag{2}$$

with colatitude θ and longitude λ. The coefficients $z_{nm}(t)$ vary with tidal periodicity. At satellite altitudes the gravitational potential of this tide is given by (e.g., Lambeck 1988)

$$U(r, \theta, \lambda, t) = 4\pi G a \rho_w \sum_{n,m} \frac{1 + k'_n}{2n+1} \left(\frac{a}{r}\right)^{n+1} z_{nm}(t)\, Y_n^m(\theta, \lambda) \tag{3}$$

where ρ_w is the mean density of sea water, a the equatorial radius of the Earth, G the gravitational constant, and k'_n are loading Love numbers.

The corresponding induced variations in the geoid are given by (e.g., Wahr et al. 1998)

$$\delta N(\theta, \lambda, t) = 3(\rho_w/\rho_e) \sum_{n,m} \left(\frac{1 + k'_n}{2n+1}\right) z_{nm}(t)\, Y_n^m(\theta, \lambda) \tag{4}$$

where ρ_e is the mean density of the Earth. As a rule of thumb, 1 cm of water column corresponds to about 1 mm in geoid. The tidal perturbations in the dimensionless Stokes coefficients $\bar{C}_{nm}$ are thus related to the elevation coefficients by

$$\delta \bar{C}_{nm} = \frac{3\rho_w}{a\rho_e} \frac{(1 + k'_n)}{(2n+1)} z_{nm}(t). \tag{5}$$

DOI: 10.2312/GFZ.b103-05088

4 Data sets used: ocean tide models CSR 4.0 and FES2004

Both ocean tide models are given in spherical harmonic form for the present purpose, in units of [cm water]. Thus, the tabulated constants primarily give the tidal elevation ζ.

The FES series (Finite Element Solution) of ocean tidal models was developed by Ch. Le Provost et al. in Grenoble and in Toulouse. These models stem from the finite element method for the solution of the hydrodynamic equations. In situ tide gauge data from several data banks were assimilated into the model (plus TOPEX/Poseidon and ERS-2 altimetry data assimilation since the version FES99). The FES2004 data set is an update of FES2002 (Le Provost 2002), and it was received from R. Biancale, CNES, Toulouse. 17 tidal constituents are available (less than in CSR 4.0); nine of these 17 are short period tides. The FES2004 spherical harmonics are given in the Schwiderski convention (Dow 1988, McCarthy and Petit 2003). They are fully normalized. The perturbations (terms) for the short period tides are tabulated up to (n=80, m=80). The annual Sa and the semi-annual Ssa tides are modelled hydrodynamically. Further long period tides (Mm, Mf, Mtm, MSqm) are from FES2002 up to (50,50). The equilibrium Om1/Om2 tides (nodal tides, with P=18.6 a and P=9.3 a) are present only with their (n=2, m=0) terms. Only the perturbations with $n \geq 2$ were used. Atmospheric tides are not included in this model. (They enter the AOD products through the ECMWF atmospheric model data.) Table 2 shows the 17 tidal constituents contained in the FES2004 data file. The phase correction χ_s is explained in Appendix A.

CSR 4.0 (Eanes 2002) from Center for Space Research, Austin, Texas, is an empirical model obtained from TOPEX/Poseidon altimetry with the model FES94.1 as the reference model. The principles of modeling are described in Eanes and Bettadpur (1995). Apart from the 17 tides mentioned above, CSR 4.0 contains some more tides, which could not be used in this study. The degree and order is different for different tidal constituents, maximally up to n=m=50. CSR 4.0 is provided as unnormalized ocean tide height harmonics (cf. McCarthy and Petit 2003: IERS Conventions 2003, chapter 6). Atmospheric tidal contributions at the S_2 period were omitted. The CSR 4.0 data file was converted to the Schwiderski convention by J.-Cl. Raimondo, GFZ Potsdam, and it was fully normalized (Heiskanen and Moritz 1967).

DOI: 10.2312/GFZ.b103-05088

Table 2: 17 tidal constituents of the FES2004 model

Tide	Doodson number	χ_s [°]	Period [d]
Om1	55.565	+180	6798.36
Om2	55.575	0	3399.18
Sa	56.554	0	365.26
Ssa	57.555	0	182.62
Mm	65.455	0	27.56
Mf	75.555	0	13.66
Mtm	85.455	0	9.13
MSqm	93.555	0	7.096
Q_1	135.655	+270	1.1195
O_1	145.555	+270	1.0758
P_1	163.555	+270	1.0027
K_1	165.555	+90	0.9973
$2N_2$	235.755	0	0.5377
N_2	245.655	0	0.5274
M_2	255.555	0	0.5175
S_2	273.555	0	0.5000
K_2	275.555	0	0.4986

Fig. 1 and 2 show degree variances of model differences, for short period and long period tides, respectively, expressed as [cm water], i.e. as z_{nm}. The prograde and retrograde parts are shown separately. 'Prograde' means travelling westward (following the tide-raising body). This is contrary to the definition of prograde in Earth rotation theory. The prograde spectra are greater than the retrograde parts. In the long period tides, some perturbations have differences around 0.1 cm of water, especially the (2,0) terms of several tides.

DOI: 10.2312/GFZ.b103-05088

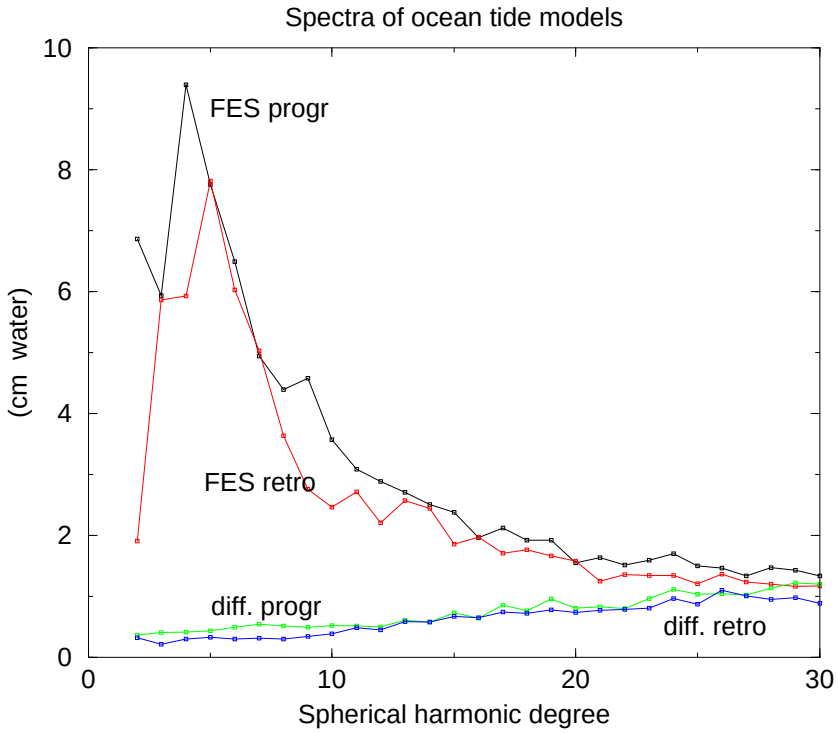

Figure 1: Spherical harmonic spectra of the ocean tide model FES2004 and the difference (FES2004 minus CSR 4.0) for nine short period tides. 'diff. progr' means the prograde part of the difference. 'retro' means retrograde.

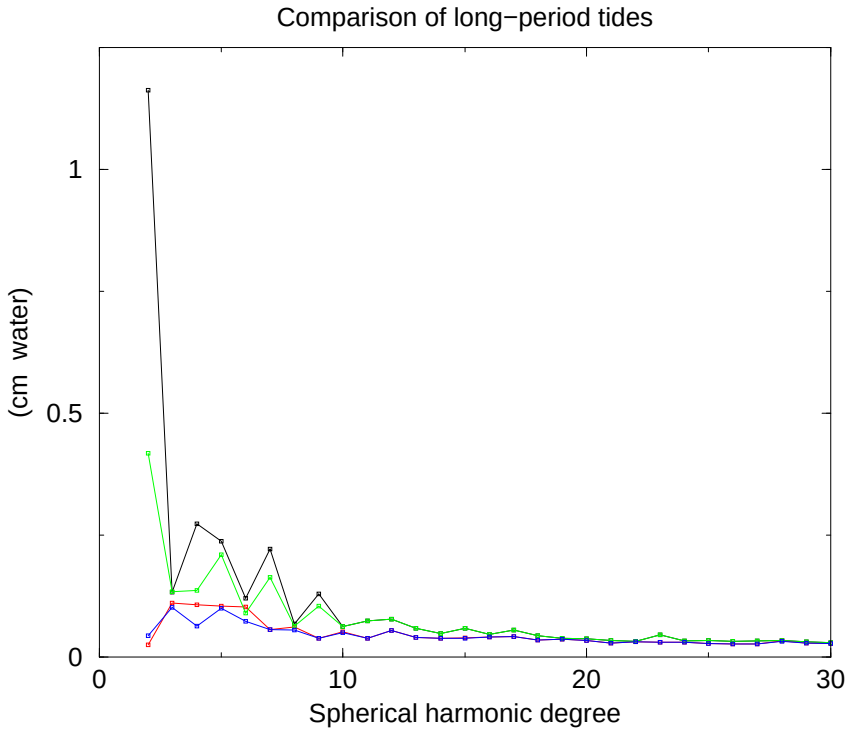

Figure 2: Spherical harmonic spectra of the ocean tide model FES2004 and the difference (FES2004 minus CSR 4.0) for eight long period tides. Black: FES2004 prograde; red: FES2004 retrograde; green: difference prograde; blue: difference retrograde.

DOI: 10.2312/GFZ.b103-05088

5 Calculations of ocean tide effects

Appendix A lists some important relations concerning the astronomical argument of tidal constituents and the summation of ocean tidal harmonics.

5.1 Monthly means of tidal elevation differences

Monthly **averages** of both ocean tide models for August and May, 2003, were formed with a time step of 6 h (N=124 points in time), up to n=m=30. Thus, S_2 (P=12.0000 h) should be completely reduced to zero if N is even, which is the case. We averaged ocean tidal elevations z_{nm} in time, transformed z_{nm} to geoid heights δN (equ. 4), then formed the difference of both averages (FES2004 minus CSR 4.0). Note that not all tidal constituents are defined completely up to (30,30) in CSR 4.0. (This is not a problem. It simply means that this model has the value of 0 at some (n,m).) The monthly mean of the eight *long period tides* ranges from –0.33 to +0.17 mm geoid for May and from –0.20 to +0.42 mm geoid for August, 2003 which cannot be neglected without further consideration. The negative extremum in geoid height differences occurs near the North pole, the positive extremum near the South pole. Near the equator and in the tropics, an n=4 sectorial pattern is visible.

Graphical presentations for the sum of nine *short period tides* from Table 2 (May and August, 2003) were also produced. Their range is from –0.016 to +0.037 mm geoid (May) and –0.015 to +0.012 mm geoid (August). The extrema arise in Antarctica (Ross Sea and Wedell Sea) and, for example, in the Sea of Okhotsk. Also, extremal values are reached between Australia and New Zealand and between Greenland and Canada, cf. Fig. 3 and 4. However, all short period differences are rather small.

5.2 Orbital simulations

We now turn to a more realistic study of the influence of ocean tide model errors. The structure of these simulations is the following: We used orbit data of the GRACE A satellite. Cartesian coordinates $x(t), y(t), z(t)$ in the Earth-fixed reference frame (co-rotating frame) were transformed into spherical coordinates $r(t)$, $\lambda(t)$, $\varphi(t)$ with longitude λ and latitude φ. Having constructed a data file of ocean tide model differences, we sum up the ocean tidal elevation differences Δz_{nm} (FES2004 minus CSR 4.0) up to n=m=10 (M_2, S_2, O_1, K_1) or n=m=30 (K_2, N_2, $2N_2$, P_1, Q_1 and a computation for the sum of nine short period tides) with a time step of $\Delta t = 60$ s. Now we transform from Δz_{nm} to dimensionless Stokes coefficients (equ. 5 and Appendix A) using numerical values of a, M, ρ_w according to CSR 4.0 (equatorial radius $a = 6378.145$ km, mass of the Earth $M = 5.97423 \cdot 10^{24}$ kg, mean density of sea water $\rho_w = 1025$ kg/m^3) and

DOI: 10.2312/GFZ.b103-05088

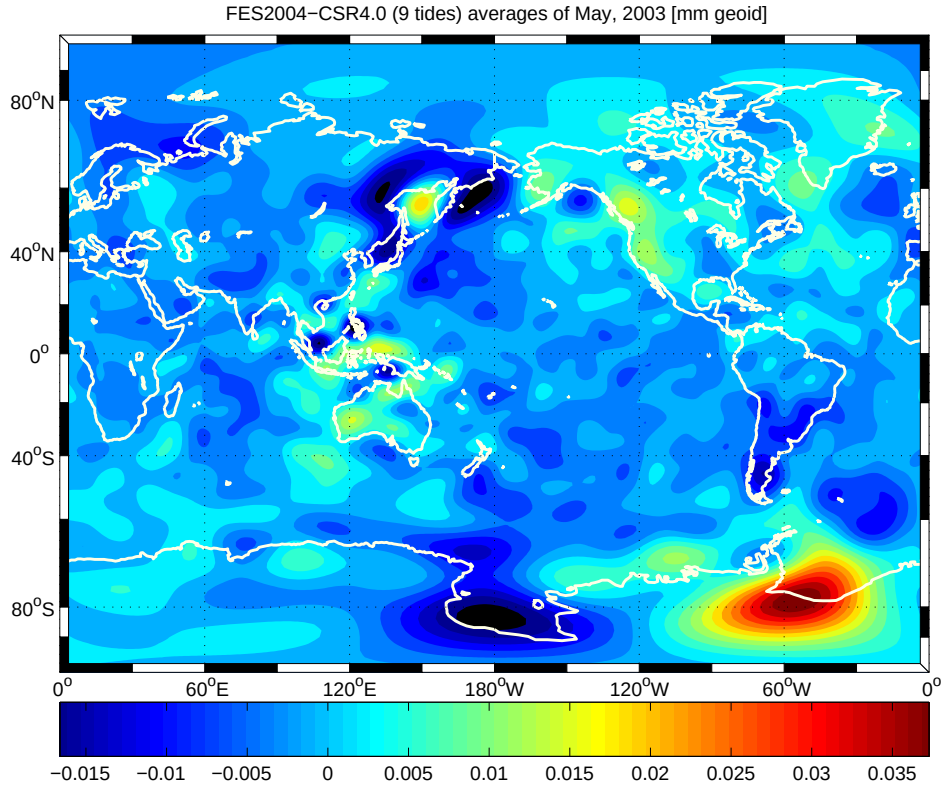

Figure 3: Difference of monthly averages for the two tidal models considered (9 short period tides) for May, 2003. Units are [mm geoid].

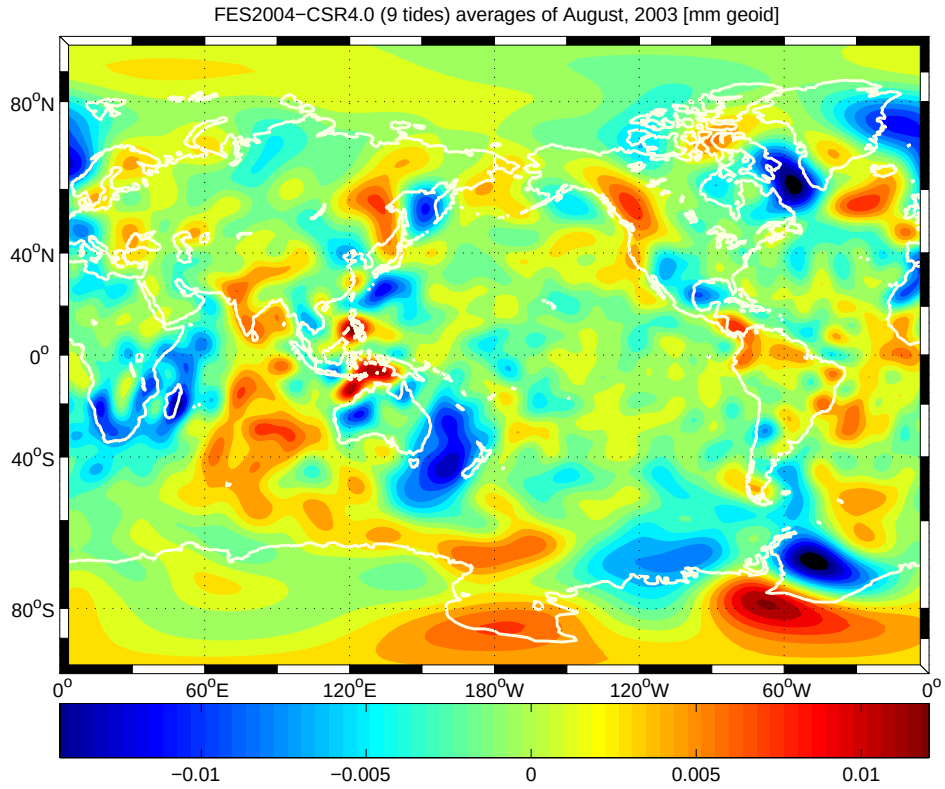

Figure 4: Difference of monthly averages for the considered tidal models (9 short period tides) for August, 2003.

DOI: 10.2312/GFZ.b103-05088

loading Love numbers k'_n according to Gegout (1997). Thus, ocean tidal loading enters at this point. Then we perform a spherical harmonic *synthesis* on the sphere at the footpoints of GRACE A. (The footpoint is the point at the spherical "Earth's surface" radially below GRACE A). Thus, we obtain geoid height differences ΔN (Torge 2003, Ilk et al. 2005), according to equation (4) above. This time series of $\Delta N(t)$ comprises, for example, 31 days in August 2003, with N = 31·24·60 = 44640 points along the orbit. Then, we formed block averages in the footpoint coordinates λ, φ on a $3^\circ \times 3^\circ$ grid from the $\Delta N(\lambda(t), \varphi(t))$ values (from a time series to block averages; i.e., resampling). On the average, there are 44640/(120·60) = 6.2 footpoints per block (actually from 1 to 11, a chess-board pattern). Plots (maps) of these block averages were produced. Also, the block averages were expanded into spherical harmonics up to degree n=60 and degree variances σ_n were formed:

$$\sigma_n = a \cdot \Big(\sum_{m=2}^{n} (\delta \bar{C}_{nm}^2 + \delta \bar{S}_{nm}^2) \Big)^{1/2} \tag{6}$$

The maps (Fig. 5–9) show the results of the orbital simulations. The patterns are obviously to some extent influenced by the Gibbs phenomenon.

DOI: 10.2312/GFZ.b103-05088

6 Results and visualization

The graphical presentations of differences between the two considered ocean tide models (orbital simulations) for August, 2003, are grouped as follows: a) individual short period tides: O_1, S_2, K_2, (not shown: M_2, N_2, $2N_2$, K_1, P_1, Q_1); b) the sum of nine short period tides from Table 2; c) the long period Mf tide.

First, the O_1 pattern is presented as typical (Fig. 5). The O_1, K_1 and M_2 maps have small scale features (neighbouring $3° \times 3°$ blocks are alternating in the sign of ΔN). Often, neighbouring North-South stripes show alternating signs.

The differences in O_1 show the following extrema: maxima and minima (red and blue) are near the coast of Antarctica (especially from 0° to 180° W), a broad region around Sulawesi, and finally in the Bering Sea.

Table 3 lists area-weighted means and standard deviations (weighting with $\cos\varphi$; N = 7200 blocks) for August, 2003. Additionally, for S_2 and K_2 the results for May, 2003 are listed, too, because of long alias periods.

Table 3: Statistics for area-weighted block averages of the orbital simulations

Tide, Month	Weighted mean [mm geoid]	Minimum [mm geoid]	Maximum [mm geoid]	Weighted std. dev. [mm geoid]
Semidiurnal tides:				
M_2 August	0.0037	-1.96	2.12	0.212
S_2 May	0.0584	-0.91	0.77	0.257
S_2 August	-0.0351	-0.74	0.93	0.262
N_2 August	0.0002	-0.62	0.99	0.069
K_2 May	-0.0168	-0.83	0.84	0.232
K_2 August	-0.0258	-0.88	1.02	0.238
$2N_2$ August	0.0013	-0.33	0.30	0.047
Diurnal tides:				
K_1 August	0.0019	-0.94	1.09	0.069
O_1 August	0.0001	-1.49	1.17	0.111
P_1 August	0.0001	-0.70	0.82	0.057
Q_1 August	0.0005	-0.24	0.47	0.038
Sum of 9 tides, August	-0.0498	-2.61	7.16	0.562
Long period tides:				
Mtm August	0.0001	-0.19	0.27	0.018
Mf August	-0.0009	-1.07	1.10	0.106
Mm August	-0.0002	-0.34	0.34	0.033

DOI: 10.2312/GFZ.b103-05088

From Table 3 we note that the maximum of the sum of nine short period tides is very large (it occurs in a region of Antarctica), and maximum and minimum are asymmetric (skewness). The weighted standard deviations are very small for N_2, $2N_2$, K_1, P_1, Q_1, Mtm and Mm, very large for the sum of nine short period tides.

Let us comment the distribution of the extrema for individual tides. S_2 and K_2 (Figure 6 and 7) do not show stripes but large scale features. S_2 has a very regular pattern, mainly of degree n=4. The global maximum occurs in Antarctica, near the Antarctic peninsula. For S_2 the coefficients $\bar{S}_{42}$, $\bar{C}_{44}$ and $\bar{S}_{44}$ in the expansion of the ΔN surface in spherical harmonics are large. Maximum differences in K_2 (red) appear west and east of New Zealand, west of Greenland, in the Bering Sea, in the Wedell Sea and in India and the Bay of Bengal. Strangely, there is also a maximum in western Australia. Minima (blue) for K_2 are seen in the equatorial Pacific, east of South Africa and in the Hudson Bay. The structures on the K_2 map are of a smaller scale than those on the S_2 map.

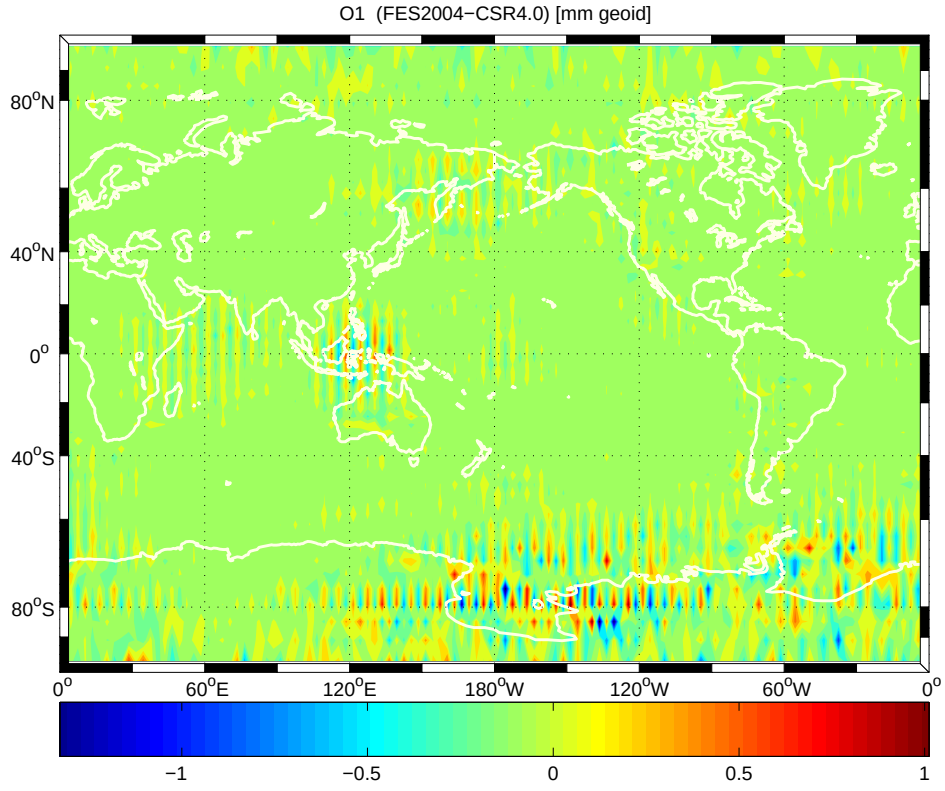

Figure 5: The result of the orbital simulation for O_1 (August 2003). Units are [mm geoid].

Let us recall the aliasing periods for S_2 (162.2 d) and K_2 (1460 d) according to Knudsen (2003) (cf. Table 1). In addition to August 2003, model differences in S_2 and K_2 were also simulated for May 2003. The S_2 pattern for May (not shown) is nearly opposite in sign compared to the one for August (Fig. 6); the time difference of 92 d between

DOI: 10.2312/GFZ.b103-05088

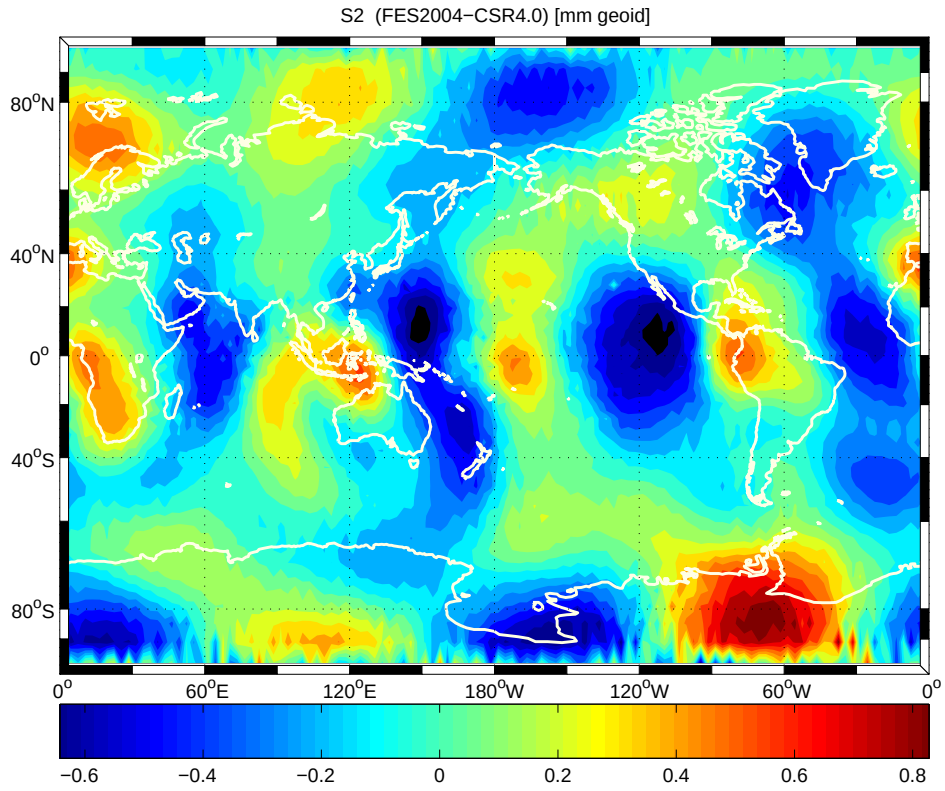

Figure 6: The result of the orbital simulation for S_2 (August 2003).

May and August compares well to half the aliasing period (81 d). This supports the interpretation as an aliasing phenomenon. K_2 for May is nearly unchanged compared to August (red and blue areas).

For the diurnal K_1 tide, greater differences (FES2004 minus CSR 4.0) occur only near the poles and north of Norway.

Although the weighted standard deviation for M_2 is rather large (Table 3), the structures for M_2 are of a small spatial scale and do not lead to large degree variances (see below). M_2 shows maxima and minima in Antarctica (0° to 120° W), around northwest Canada and Alaska, around the Philippines, in the vicinity of South Africa and west of Spain.

The maxima and minima of N_2 occur in Antarctica (south of the Antarctic peninsula), east of the tip of South America, north of Kola and west of Greenland. For N_2, the area-weighted standard deviation is very small.

Fig. 8 displays the differences between the two tidal models for the sum of nine short period tides (for August 2003) resulting from orbital simulation. Note that these differences are much larger than those presented in Fig. 4 due to unfavourable distribution of sampling and should be considered in the processing of GRACE data. Fig. 8 shows one large maximum in Antarctica (south of the Antarctic peninsula). However, this area

DOI: 10.2312/GFZ.b103-05088

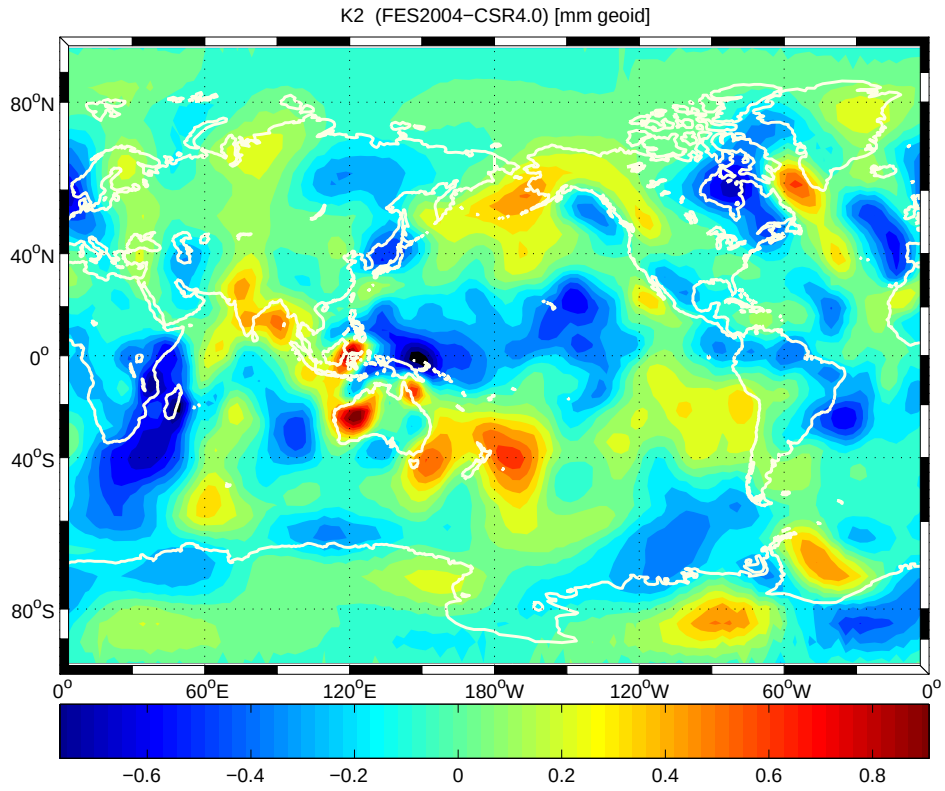

Figure 7: The result of the orbital simulation for K_2 (August 2003).

in Antarctica is small, due to the convergence of the meridians. Another maximum occurs around Sulawesi, and one more in north west Canada, see Figure 8. Two regions of minima occur in the equatorial Pacific (one of them near Papua New Guinea), furthermore in Hudson Bay, and a minimum east of South Africa. There is also a kind of minimum near the Ross Sea.

Our simulation of the long period Mf tide (P=13.66 d) shows extrema mainly in the Arctic ocean (Fig. 9).

Graphical presentations of degree variances (equ. 6) and comparison with the GRACE accuracy (GRACE 'baseline' (in red) and the presently achievable actual accuracy (in green)) can be found in Fig. 10 for S_2, in Fig. 11 for K_2 and in Fig. 12 for the sum of nine short period tidal constituents. S_2 has a strong upward spike at n=4. The sum of nine tides appears to be dominated by the sum of S_2 plus K_2.

Table 4 lists the limits of accuracy. Below spherical harmonic degree n_1 ($n \leq n_1$) the simulated ocean tide errors are larger than the GRACE errors (present GRACE accuracy, green line in Fig. 10–12). Below n_b ($n \leq n_b$) the ocean tide errors are larger than the noise represented by the GRACE baseline (red line in Fig. 10–12). Note that these degree variances are based on $3° \times 3°$ block means. They would be somewhat larger for $2° \times 2°$ block means and nearly halved for $6° \times 6°$ block means ('smoothing').

DOI: 10.2312/GFZ.b103-05088

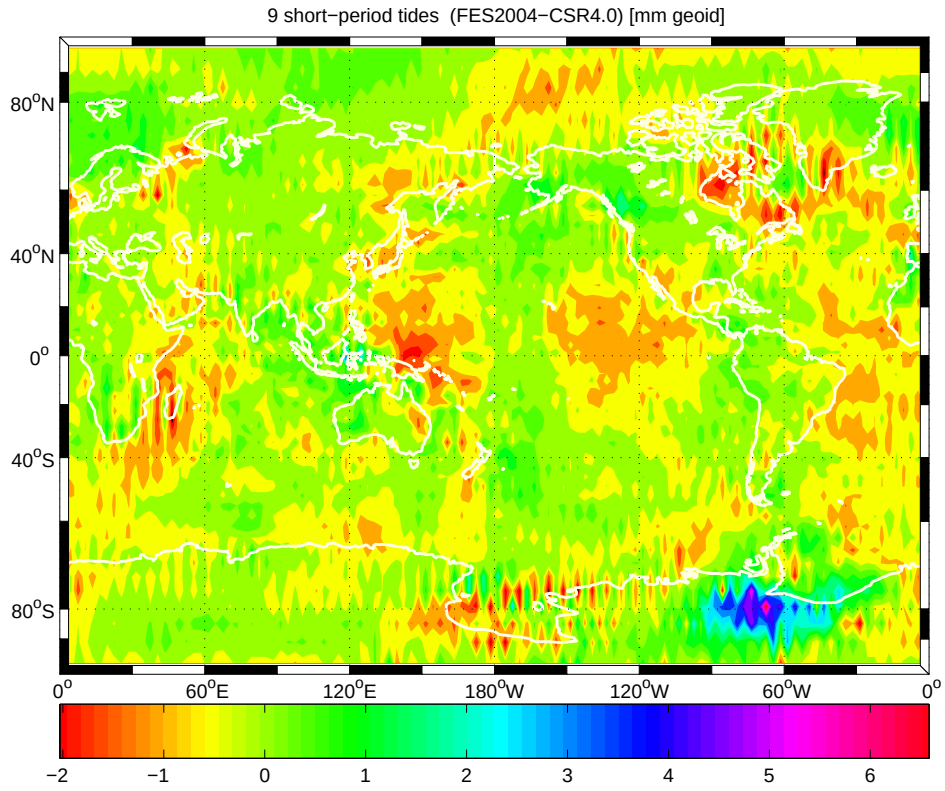

Figure 8: The result of the orbital simulation for the sum of nine short period tides, August 2003. Note that the color palette is different from the previous figures.

Table 4: Limits of accuracy derived from the orbital simulations

Tide	n_1	n_b
S_2	7	16
K_2	8	26
Sum of 9 tides	15	34

The degree variances of the other individual tide differences between the two ocean tide models have the following features. The values for M_2 are near or below the red line (GRACE baseline). Only the points for n=4 and n=6 are about 20 percent above the baseline curve. K_1 touches the baseline curve from below at n=27. O_1 lies entirely below the baseline curve. The degree variances for N_2 are very small and almost invisible in such a plot.

Knudsen and Andersen (2004, 'Improving S_2 ocean tides using GRACE gravimetry', Joint CHAMP/GRACE Science Meeting Potsdam, in preparation for Proceedings) attempt to improve the modelling of the oceanic S_2 tide using 15 GRACE months and fitting a period of P=163d in time (the aliasing period of S_2 for GRACE).

DOI: 10.2312/GFZ.b103-05088

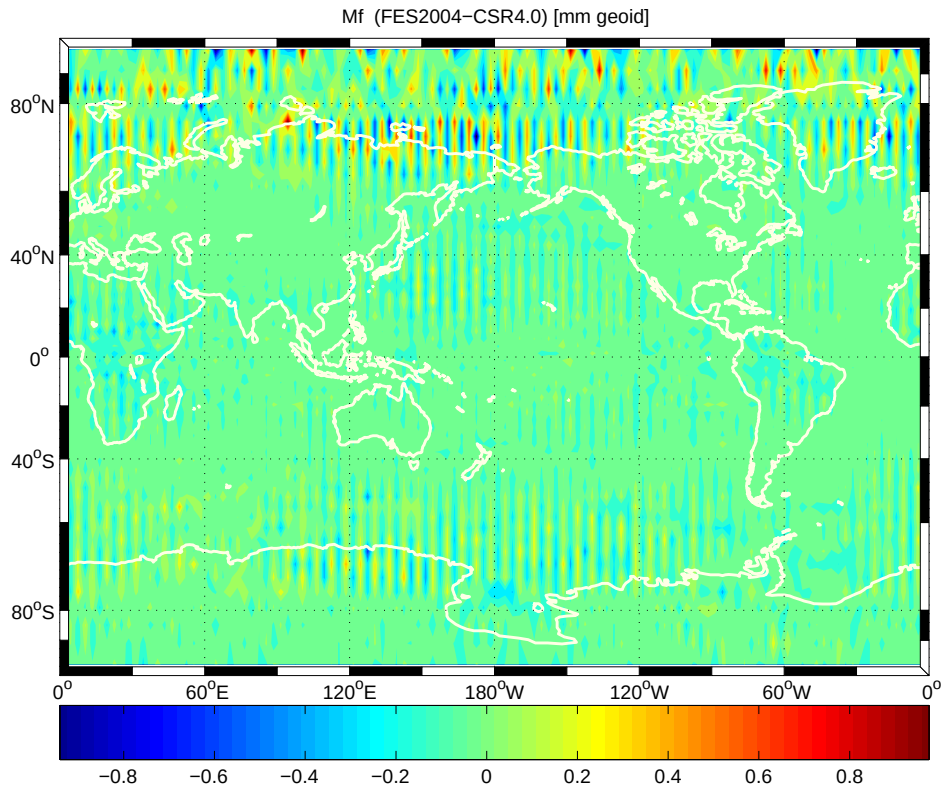

Figure 9: The result of the orbital simulation for the long period Mf tide (P=13.66 d), August 2003.

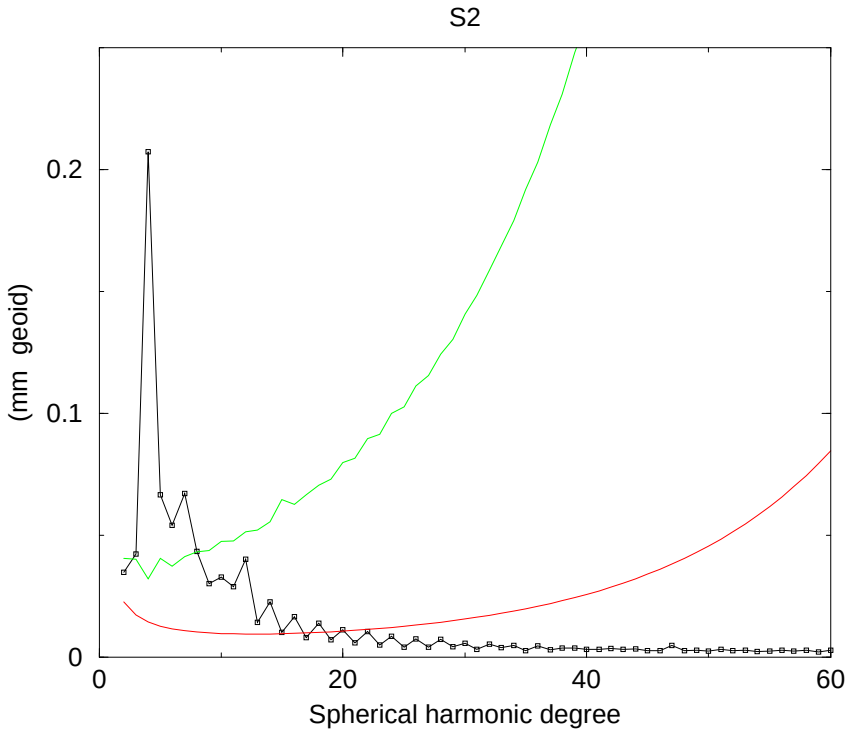

Figure 10: Degree variances for the S_2 resulting from orbital simulation. Red line = GRACE baseline; green line = present GRACE accuracy.

GeoForschungsZentrum Potsdam Scientific Technical Report STR 05/08
DOI: 10.2312/GFZ.b103-05088

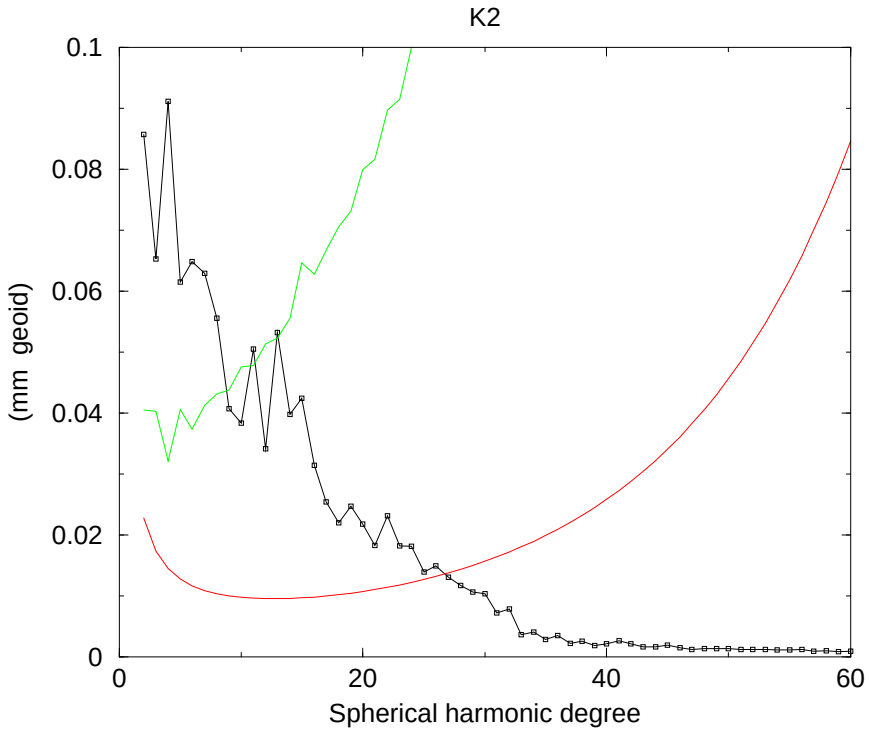

Figure 11: Degree variances for the K_2 orbital simulation, GRACE baseline (red) and present GRACE accuracy (green).

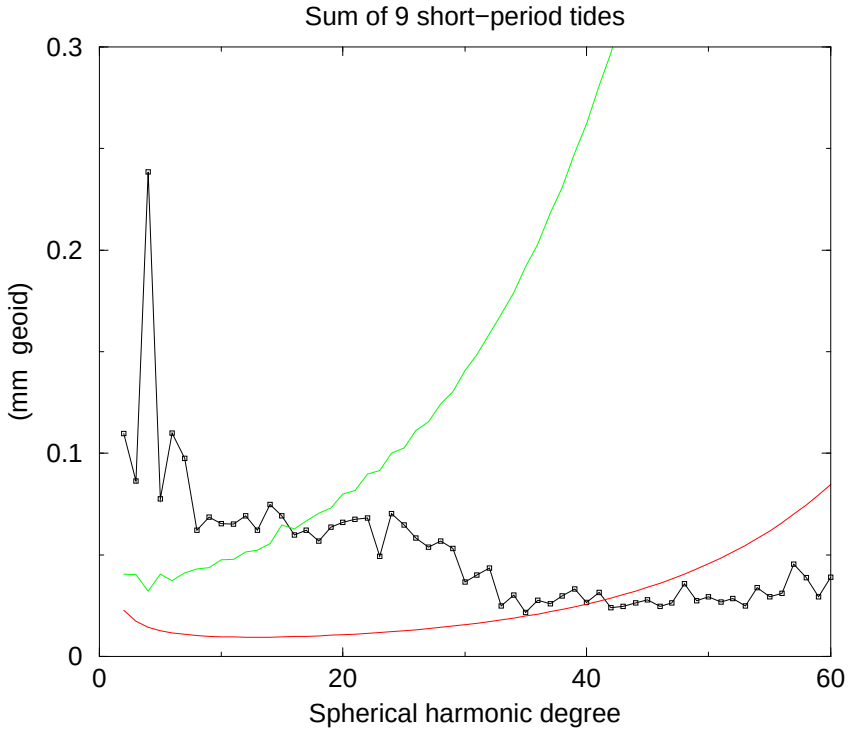

Figure 12: Degree variances resulting from the orbital simulation for the sum of nine short period tidal constituents, GRACE baseline (red) and present GRACE accuracy (green).

DOI: 10.2312/GFZ.b103-05088

7 Conclusions

- The sum of nine short period tides illustrates well that although the differences in monthly averages appear to be negligible, the orbital simulation can prove obvious aliasing effects.

- In the preceding section we outlined the accuracy limits for the tides S_2 and K_2 and for the sum of nine short period tides. Comparing with Han et al. (2004), we note that the conclusions are similar, although Han used only the GRACE baseline curve and did not simulate K_2. The deviation of the two presently used ocean tide models from reality is at least of the same order of magnitude as the difference between the two models.

- On the other hand, M_2, K_1 and O_1 cause no problems for GRACE according to our simulations due to their small spatial scale.

- Only the S_2 and K_2 short period tidal constituents could represent a problem for GRACE data analysis since they have long alias periods.

- The influence of long period constituents cannot be neglected in the montly means of model differences and requires further investigation. Relatively little is known about the nodal tides Om1, Om2 (P=18.6 a and P=9.3 a). Usually, an equilibrium tidal behaviour is assumed for these.

- The modelling of ocean tides in Hudson Bay, Bering Sea, the Gulf of Alaska, the Sea of Okhotsk, Yellow Sea, Ross Sea etc. can still be improved in the models.

- The representation of tides in areas beyond the maximal latitudes ($\approx \pm 66°$) of the TOPEX/Poseidon satellite is problematic according to our calculations, especially near Antarctica. The combination of TOPEX and Jason altimetry data may further improve empirical models of ocean tides.

- The ocean tides around Antarctica are further influenced by the seasonal cycle and interannual variations of *sea ice*.

DOI: 10.2312/GFZ.b103-05088

Acknowledgements

The German Ministry of Education and Research (BMBF) supports the GRACE Science Data System at GFZ within the Geotechnologien geoscientific R+D programme under grant 03F0326A.

The authors are grateful for discussions with and/or data from L. Ballani (GFZ), F. Barthelmes (GFZ), R. Biancale (CNES, Toulouse), F. Flechtner (GFZ), R. Hengst (GFZ), U. Meyer (GFZ), J.-Cl. Raimondo (GFZ), J. Ries (CSR, Austin), R. Schmidt (GFZ).

M_Map for MATLAB, written by R. Pawlowicz, was used for producing maps.

DOI: 10.2312/GFZ.b103-05088

References

Allaby A. and Allaby M., eds., 1999. 'A Dictionary of Earth Sciences', Oxford University Press. Oxford Reference Online, Oxford University Press

Bartels J., 1957. 'Gezeitenkräfte', in: Handbuch der Physik, Flügge S., ed., Band 48, Geophysik II, pp. 734–774

Boy J.-P. and Chao B. F., 2002. 'Time-variable gravity signal during the water impoundment of China's Three-Gorges Reservoir', Geophys. Res. Lett. 29, 2200, doi:10.1029/2002GL016457

Brigham E. O., 1992. 'FFT, Schnelle Fourier-Transformation', 5. Auflage, R. Oldenbourg Verlag, München, Wien

Cartwright, D. E. and Tayler, R. J., 1971, 'New Computations of the Tide-Generating Potential', Geophys. J. Roy. astr. Soc., 23, 45–74

Chambers D. P., Wahr J. and Nerem R. S., 2004. 'Preliminary observations of global ocean mass variations with GRACE', Geophys. Res. Lett. 31, L13310, doi:10.1029/2004GL020461

Cheng M. K., 2002. 'Gravitational perturbation theory for intersatellite tracking', J. Geodesy 76, 169–185

Dickey J. and National Research Council Commission (NRC), 1997. 'Satellite gravity and the geosphere', National Academy Press, Washington DC, pp. 112

Dobslaw H., Schwintzer P., Barthelmes F., Flechtner F., Reigber Ch., Schmidt R., Schöne T. and Wiehl M., 2004. 'Geostrophic ocean surface velocities from TOPEX altimetry, and CHAMP and GRACE satellite gravity models', Scientific Technical Report STR04/07, GFZ Potsdam, pp. 22

Döll P., Kaspar F. and Lehner B., 2003. 'A global hydrological model for deriving water availability indicators: model tuning and validation', Journal of Hydrology 270, 105–134

Doodson A. T., 1921. 'The Harmonic Development of the Tide-Generating Potential', Proc. R. Soc. A., 100, 305–329

Dow J. M., 1988. 'Ocean Tides and Tectonic Plate Motions from Lageos', Dissertation, DGK Reihe C, Nr. 344

Eanes R., 2002. 'The CSR4.0 Global Ocean Tide Model', ftp://www.csr.utexas.edu/pub/tide

Eanes R. and Bettadpur S., 1995. 'The CSR 3.0 global ocean tide model', Tech. Memo. CSR–TM–95–06, Cent. for Space Res., Univ. of Tex., Austin

DOI: 10.2312/GFZ.b103-05088

Eubanks T. M., McCarthy D. D., Luzum B. J. and Ray J. R., 1995. 'Observation of rapid polar motions induced by an atmospheric normal mode', NASA DOSE workshop, November 1995

Fan Y. and van den Dool H., 2004. 'Climate Prediction Center global monthly soil moisture data set at 0.5° resolution for 1948 to present', J. Geophys. Res. 109, D10102, doi:10.1029/2003JD004345

Flechtner F., 2003. 'AOD1B Product Description Document', GRACE Project Documentation, JPL 327–750, Rev. 1.0, JPL, Pasadena, Ca.

Fleming K., Martinec Z. and Hagedoorn J., 2004. 'Geoid displacement about Greenland resulting from past and present-day mass changes in the Greenland Ice Sheet', Geophys. Res. Lett. 31, L06617, doi:10.1029/2004GL019469

Gegout P., 1997. Loading Love numbers, private communication

Gross R. S. and Chao B. F., 2001. 'The gravitational signature of earthquakes', in: M. G. Sideris, ed., Gravity, geoid and geodynamics 2000. IAG Symp. Vol. 123, Springer-Verlag, Berlin, p. 205–210

Han S.–C., Jekeli C. and Shum C. K., 2004. 'Time-variable aliasing effects of ocean tides, atmosphere, and continental water mass on monthly mean GRACE gravity field', J. Geophys. Res. 109, B04403, doi:10.1029/2003JB002501

Heiskanen W. A. and Moritz H., 1967. 'Physical Geodesy', W. H. Freeman, San Francisco, CA

Ilk K. H., Flury J., Rummel R., Schwintzer P., Bosch W., Haas C., Schröter J., Stammer D., Zahel W., Miller H., Dietrich R., Huybrechts P., Schmeling H., Wolf D., Götze H. J. Riegger J., Bardossy A., Güntner A. and Gruber Th., 2005. 'Mass Transport and Mass Distribution in the Earth System', Contribution of the New Generation of Satellite Gravity and Altimetry Missions to Geosciences, Proposal for a German Priority Research Program, 2nd Edition, GOCE-Projektbüro Deutschland, TU München, GFZ Potsdam

Kaban M. K., Schwintzer P. and Reigber Ch., 2004. 'A new isostatic model of the lithosphere and gravity field', J. Geodesy 78, 368–385

Kanzow T., Flechtner F., Chave A., Schmidt R., Schwintzer P. and Send U., 2005. 'Seasonal variation of ocean bottom pressure derived from GRACE: Local validation and global patterns', accepted by Geophys. Res. Lett.

Knudsen P., 2003. 'Ocean Tides in GRACE Monthly Averaged Gravity Fields', Space Science Reviews 108 (1–2), 261–270

Knudsen P. and Andersen O., 2002. 'Correcting GRACE gravity fields for ocean tide effects', Geophys. Res. Lett. 29, No. 8, 10.1029/2001GL014005

Lambeck K., 1998. 'Geophysical Geodesy', Clarendon Press, Oxford

Le Provost, C., 2002. 'FES2002 – A New Version of the FES Tidal solution Series', Abstract Volume, Jason–1 Science Working Team Meeting, Biarritz, France

McCarthy D. D. and Petit G., 2003. 'IERS Conventions 2003', http://maia.usno.navy.mil/conv2003.html

Milly P. C. D. and Shmakin A. B., 2002. 'Global Modeling of Land Water and Energy Balances. Part I: The Land Dynamics (LaD) Model', Journal of Hydrometeorology 3, 283–299

Morris Ch.,ed., 1992. 'Academic Press dictionary of science and technology', Academic Press, San Diego

Peters T., 2001. 'Zeitliche Variationen des Gravitationsfeldes der Erde', diploma thesis, TU München, IAPG/FESG No. 12

Ray R. D., Eanes R. J., Egbert G. D. and Pavlis N. K., 2001. 'Error spectrum for the global M_2 ocean tide', Geophys. Res. Lett. 28, 21–24

Ray R. D., Rowlands D. D. and Egbert G. D., 2003. 'Tidal models in a new era of satellite gravimetry', Space Science Reviews 108 (1–2), 271–282

Reigber C., Schmidt R., Flechtner F., König R., Meyer U., Neumayer K.–H., Schwintzer P. and Zhu S. Y., 2004. 'An Earth Gravity Field Model Complete to Degree and Order 150 from GRACE: EIGEN–GRACE02S', J. of Geodynamics, accepted

Schmidt R., Schwintzer P., Flechtner F., Reigber C., Güntner A., Döll P., Ramillien G., Cazenave A., Petrovic S., Jochmann H. and Wünsch J., 2005. 'GRACE Observations of Changes in Continental Water Storage', accepted by Global and Planetary Change

Schwiderski E., 1983. 'Atlas of Ocean Tidal Charts and Maps, Part I: The Semidiurnal Principal Lunar Tide M_2', Marine Geodesy 6, 219–256

Tapley B. D., Chambers D. P., Bettadpur S. and Ries J. C., 2003. 'Large scale ocean circulation from the GRACE GGM01 Geoid', Geophys. Res. Lett. 30, 2163, doi:10.1029/2003GL018622

Tapley B. D., Bettadpur S., Watkins M. and Reigber Ch., 2004a. 'The gravity recovery and climate experiment: Mission overview and early results', Geophys. Res. Lett. 31, L09607, doi:10.1029/2004GL019920

Tapley B. D., Bettadpur S., Ries J. C., Thompson P. F. and Watkins M. M., 2004b. 'GRACE measurements of mass variability in the Earth system', Science 305, 503–505

Thompson P. F., Bettadpur S. V. and Tapley B. D., 2004. 'Impact of short period, non-tidal, temporal mass variability on GRACE gravity estimates', Geophys. Res. Lett. 31, L06619, doi:10.1029/2003GL019285

Torge W., 2003. 'Geodäsie', 2. Auflage, de Gruyter, Berlin, New York

Velicogna I. and Wahr J., 2002. 'Postglacial rebound and Earth's viscosity structure from GRACE', J. Geophys. Res. 107 (B12), 2376 doi:10.1029/2001JB001735

Wahr J. M., Molenaar M. and Bryan F., 1998. 'Time variability of the Earth's gravity field: Hydrological and oceanic effects and their possible detection using GRACE', J. Geophys. Res. 103 (B12), 30205–30229

Wahr J., Swenson S., Zlotnicki V. and Velicogna I., 2004. 'Time-variable gravity from GRACE: First results', Geophys. Res. Lett. 31, L11501, doi:10.1029/2004GL019779

Wiehl M. and Dietrich R., 2005. 'Time-variable gravity seen by satellite missions: on its sampling and its parametrization'. In: Reigber C., Lühr H., Schwintzer P., Wickert J. (Eds.), Earth Observation with CHAMP – Results From Three Years in Orbit, Springer, Heidelberg

Wilhelm H. and Zürn W., 1984. 'Tidal Forcing Field', in: Fuchs K., Soffel H. (eds.), Landolt-Börnstein V/2a, Geophysics of the Solid Earth, the Moon and the Planets, Springer, Berlin, pp. 261–279

Wilks D. S., 1995. 'Statistical methods in the atmospheric sciences: an introduction', Academic Press, San Diego

Wunsch C. and Stammer D., 1997. 'Atmospheric loading and the oceanic inverted barometer effect', Rev. Geophys. 35, 79–107

Appendix A: Summation of the ocean tide height harmonics

According to the IERS Conventions 2003 (McCarthy and Petit 2003, chapter 6), the following definitions and relations hold. Related material can be found in Bartels (1957), Wilhelm and Zürn (1984), Dow (1988), Eanes and Bettadpur (1995).

$\bar{P}_{nm}$ is the normalized associated Legendre function related to the classical (unnormalized) one by

$$\bar{P}_{nm} = N_{nm} P_{nm}, \tag{A1a}$$

where

$$N_{nm} = \sqrt{\frac{(n-m)!(2n+1)(2-\delta_{om})}{(n+m)!}}. \tag{A1b}$$

Correspondingly, the normalized, real-valued geopotential coefficients $(\bar{C}_{nm}, \bar{S}_{nm})$ (Heiskanen and Moritz 1967) are related to the unnormalized coefficients (C_{nm}, S_{nm}) by

$$C_{nm} = N_{nm}\bar{C}_{nm}, \quad S_{nm} = N_{nm}\bar{S}_{nm}. \tag{A2}$$

In order to represent the effect of ocean tides, the astronomical argument θ_s of the tidal constituent s is needed:

$\theta_s = \bar{n} \cdot \bar{\beta} = \sum_{i=1}^{6} n_i \beta_i$, or $\theta_s = m(\theta_g + \pi) - \bar{N} \cdot \bar{F} = m(\theta_g + \pi) - \sum_{j=1}^{5} N_j F_j$,

where

$\bar{\beta}$ = six-vector of Doodson's fundamental arguments β_i, (τ, s, h, p, N', p_s) [Wilhelm and Zürn 1984],

$\bar{n}$ = six-vector of multipliers n_i (for the term at frequency f) of the fundamental arguments,

$\bar{F}$ = five-vector of fundamental arguments F_j (the Delaunay variables l, l', F, D, Ω) of nutation theory,

$\bar{N}$ = five-vector of multipliers N_i of the Delaunay variables for the nutation of frequency $-f + d\theta_g/dt$,

and θ_g is the Greenwich Mean Sidereal Time expressed in angle units (*i.e.* $24^h = 360°$).

Effect of the Ocean Tides:

The dynamical effects of ocean tides are most easily incorporated as periodic variations

DOI: 10.2312/GFZ.b103-05088

of the normalized Stokes' coefficients. These variations can be written as

$$\Delta\bar{C}_{nm} - i\Delta\bar{S}_{nm} = F_{nm} \sum_{s(n,m)} \bar{\sum_{+}} (C^{\pm}_{snm} \mp iS^{\pm}_{snm}) e^{\pm i\theta_s}, \qquad (A3)$$

where

$$F_{nm} = \frac{4\pi G\rho_w}{g_e} \sqrt{\frac{(n+m)!}{(n-m)!(2n+1)(2-\delta_{om})}} \left(\frac{1+k'_n}{2n+1}\right),$$

g_e = mean equatorial gravity, G = the gravitational constant, ρ_w = mean density of sea water = 1025 kg m^{-3},

k'_n = load deformation coefficients ($k'_2 = -0.3054, k'_3 = -0.196, k'_4 = -0.134,\ k'_5 = -0.1047, k'_6 = -0.0903,$ etc.) according to Gegout (1997),

$C^{\pm}_{snm}, S^{\pm}_{snm}$ = ocean tide coefficients (cm) for the tide constituent s,

θ_s = argument of the tide constituent s as defined above.

For our applications we replace the term $\frac{4\pi G\rho_w}{g_e}$ in the definition of F_{nm} by $\frac{4\pi a^2\rho_w}{M}$.

The summation over + and − denotes the respective addition of the retrograde waves using the top sign and the prograde waves using the bottom sign. The $C^{\pm}_{snm}$ and $S^{\pm}_{snm}$ are the coefficients of a spherical harmonic decomposition of the ocean tide height for the ocean tide due to the constituent s of the tide generating potential.

As Dow (1988), p. 48, points out, for m=0 we have $C^{+}_{sn0} = C^{-}_{sn0}$ and $S^{+}_{sn0} = S^{-}_{sn0}$ due to the construction of this expansion.

These ocean tide height harmonics are related to the Schwiderski convention (Schwiderski, 1983) by

$$C^{\pm}_{snm} - iS^{\pm}_{snm} = -i\hat{C}^{\pm}_{snm} e^{i(\epsilon^{\pm}_{snm} + \chi_s)}, \qquad (A4)$$

where $\hat{C}^{\pm}_{snm}$ = ocean tide amplitude for constituent s using the Schwiderski notation, $\epsilon^{\pm}_{snm}$ = ocean tide phase for constituent s,

and χ_s is obtained from Table A.1, with H_s being the Cartwright and Tayler (1971) amplitude at frequency s.

The real and imaginary parts of (A4) are:

$$C^{\pm}_{snm} = \hat{C}^{\pm}_{snm} \sin(\epsilon^{\pm}_{snm} + \chi_s), \qquad (A5a)$$

$$S^{\pm}_{snm} = \hat{C}^{\pm}_{snm} \cos(\epsilon^{\pm}_{snm} + \chi_s), \qquad (A5b)$$

A certain special case occurs for m=0 (zonal perturbation terms). If we transform to the Schwiderski convention, we can finally put both components into $\hat{C}^{+}_{sn0}$ and put $\hat{C}^{-}_{sn0} = 0$. This $\hat{C}^{+}_{sn0}$ is then

$$\hat{C}^{+}_{sn0} = \sqrt{C^{+2}_{sn0} + S^{+2}_{sn0}} + \sqrt{C^{-2}_{sn0} + S^{-2}_{sn0}}.$$

DOI: 10.2312/GFZ.b103-05088

Table A.1. Values of χ_s for long period, diurnal and semidiurnal tides. χ_s depends on the sign of the amplitude H_s.

Tidal Band	$H_s > 0$	$H_s < 0$
Long Period	π	0
Diurnal	$\frac{\pi}{2}$	$-\frac{\pi}{2}$
Semidiurnal	0	π

For clarity, the terms in equation (A3) are repeated in both conventions:

$$\Delta\bar{C}_{nm} = F_{nm} \sum_{s(n,m)} [(C^{+}_{snm} + C^{-}_{snm}) \cos\theta_s + (S^{+}_{snm} + S^{-}_{snm}) \sin\theta_s] \qquad (A6a)$$

or

$$\Delta\bar{C}_{nm} = F_{nm} \sum_{s(n,m)} [\hat{C}^{+}_{snm} \sin(\theta_s + \epsilon^{+}_{snm} + \chi_s) + \hat{C}^{-}_{snm} \sin(\theta_s + \epsilon^{-}_{snm} + \chi_s)], \qquad (A6b)$$

$$\Delta\bar{S}_{nm} = F_{nm} \sum_{s(n,m)} [(S^{+}_{snm} - S^{-}_{snm}) \cos\theta_s - (C^{+}_{snm} - C^{-}_{snm}) \sin\theta_s] \qquad (A6c)$$

or

$$\Delta\bar{S}_{nm} = F_{nm} \sum_{s(n,m)} [\hat{C}^{+}_{snm} \cos(\theta_s + \epsilon^{+}_{snm} + \chi_s) - \hat{C}^{-}_{snm} \cos(\theta_s + \epsilon^{-}_{snm} + \chi_s)]. \qquad (A6d)$$

The Doodson variable multipliers ($\bar{n}$) are coded into the argument number (A) after Doodson (1921) as:

$$A = n_1(n_2 + 5)(n_3 + 5).(n_4 + 5)(n_5 + 5)(n_6 + 5).$$

DOI: 10.2312/GFZ.b103-05088